Amination of Ketenes: Evidence for a Mechanism Involving Enols of Amides as Intermediates

Greet Raspoet and Minh Tho Nguyen*

Department of Chemistry, University of Leuven, Celestijnenlaan 200F, B-3001 Leuven, Belgium

Sean Kelly and Anthony F. Hegarty*

*Chemistry Department, University College Dublin, Dublin 4, Ireland*

The amination reaction of ketenes has been studied both theoretically and experimentally as a model reaction for amide bond formation. Calculations are performed using both ab initio molecular orbital theory (MO) and density functional theory (DFT) methods. Solvent effects are modeled by different methods: Onsager SCRF, PCM, and SCI-PCM electrostatic continuum solvation models, as well as explicit inclusion of actively participating water molecules, representative of a polar protic solvent, at different hydrogen bond donor−acceptor sites of the solutes. Both the concerted process and the two-step reaction, via a 1-amino-1-hydroxy ene intermediate, have been investigated at high level of theory. These intermediates are formally enols of amides. A comparison with uncatalyzed amide bond formation indicates that the active participation of a second ammonia molecule reduces the energy barrier in favor of the two-step reaction. When a water molecule acts as catalyst instead of a second ammonia molecule, this energy barrier is reduced even further, which emphasizes the catalytic role of a protic solvent molecule present in the bulk. Kinetic evidence for the formation of enols of amides has also been presented, which is consistent with the theoretical view, showing preference of a two-step reaction including the intermediacy of an enol of the amide. This enol was generated as an intermediate in the amination of the sterically hindered ketenes, bis(pentamethylphenyl) ketene and bis(mesityl) ketene, by primary and secondary amines in aprotic solvent. The kinetics of formation of the enol of the amide of these specific ketenes reveal a first-order dependency on amine concentration, and the rates of addition of several amines have been determined. The first-order rate constants suggest a reaction involving free amine molecules rather than dimers, presumably due to the low dimer concentration or to their steric bulk, and in line with the preference of amine−water complex as reactants.

Introduction

The nature of the amide functional group has long been of fundamental interest owing to its presence as a repeat unit in biological macromolecules (e.g., peptides) and industrial polymers (e.g., nylon). The reaction of ketenes **a** with ammonia or primary or secondary amines (amination) is one that has long been known[1] and yields ultimately to the corresponding amide **c** (Scheme 1).

The kinetics and mechanism of amine addition to ketenes have been studied by a number of authors and have led to several points of controversy. Satchell and co-workers[2−5] proposed a cyclic transition state, involving attack of nitrogen on the carbonyl carbon accompanied by simultaneous C_β protonation. They also suggested that the excess amine present under reaction conditions may serve as the proton-transfer reagent. Tidwell,[6] on the contrary, favored an open transition state even though a stepwise process with a zwitterionic intermediate was not explicitly proposed. In the present paper, both possibilities of an open and a cyclic transition structure are investigated. For a cyclic transition state,

Scheme 1
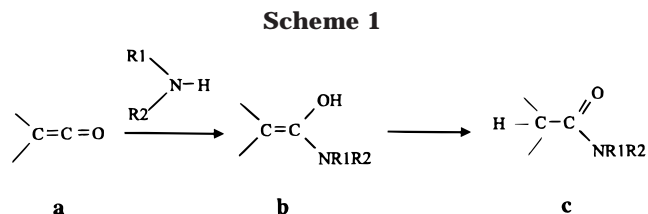
both a *concerted* reaction involving an ammonia attack across the C=C bond of ketene yielding immediately an amide **c** and a *two-step* reaction involving a nucleophilic attack of ammonia across the C=O bond of ketene proceeding via an enol amide intermediate **b** are possible reaction pathways. The "enols of amides" **b** are inherently interesting since their chemistry has received relatively little attention due to their high thermodynamic instability compared to amide isomers. Indeed, enols of amides are very elusive species, and so far, no clear evidence was found for the amide enol intermediate in the addition of amines to ketenes. However, very recently, Hegarty and co-workers[7] established the formation of an enol of an amide as an intermediate during the hydration of ketene imines which were sterically hindered at carbon. Moreover, Frey and Rappoport[8]

(1) Staudinger, H. *Die Ketene*; Enke: Stuttgart, 1912.
(2) Briody, J. M.; Satchell, D. P. N. *Tetrahedron* **1966**, *22*, 2649.
(3) Satchell, D. P. N.; Lillford, P. J. *J. Chem. Soc. B* **1967**, 360.
(4) Satchell, D. P. N.; Lillford, P. J. *J. Chem. Soc. B* **1968**, 54.
(5) Satchell, D. P. N.; Lillford, P. J. *J. Chem. Soc. B* **1969**, 1016.
(6) Seikaly, H. R.; Tidwell, T. T. *Tetrahedron* **1986**, *42*, 2587.

(7) Hegarty, A. F.; Kelly, S.; Relihan, C. M. *J. Chem. Soc., Perkin Trans 2* **1997**, 1175.
(8) Frey, J.; Rappoport, Z. *J. Am. Chem. Soc.* **1996**, *118*, 3994.

Table 1. Calculated Total Energies (hartree) and Zero-Point Vibrational (ZPE, kJ mol^{-1}) Energies for the Amination of Ketenes

	HF[a] 6-31G(d,p)	MP2[b] 6-31G(d,p)	MP2[b] 6-311++G(d,p)	QCISD(T)[b] 6-31G(d,p)	QCISD(T)[b] 6-311++G(d,p)	ZPE[c]
$H_2C=C=O$ **1**	−151.72876	−152.17629	−152.23518	−152.19528	−152.26871	81
NH_3	−56.19554	−56.38692	−56.41542	−56.40213	−56.43476	87
H_2O	−76.02361	−76.22245	−76.27491	−76.23165	−76.28684	55
1 + NH_3	−207.92430	−208.56321	−208.65060	−208.59741	−208.70347	168
TS-CC **TS2**	−207.83746	−208.48615	−208.58909	−208.53346	−208.63921	173
PC-CC **3**	−207.98898	−208.61178	−208.70928	−208.66147	−208.76195	185
RC-CO **4**	−207.92943	−208.55311	−208.65610	−208.60400	−208.70919	172
TS-CO **TS5**	−207.85810	−208.50289	−208.60518	−208.55211	−208.65669	177
PC-CO **6**	−207.94191	−208.56399	−208.66705	−208.61594	−208.72108	189
1 + 2 NH_3	−264.11984	−264.95013	−265.06602	−264.99954	−265.13823	255
RC-CO1 **7**	−264.11197	−264.94029	−265.07303	−265.00782	−265.14375	279
TS-CO1 **TS8**	−264.08920	−264.92719	−265.05951	−264.99305	−265.12886	276
PC-CO1 **9**	−264.15078	−264.96585	−265.09838	−265.03570	−265.17122	283
1 + NH_3 + H_2O	−283.94791	−284.78566	−284.92551	−284.82906	−284.99031	223
RC-CO2 **10**	−283.94259	−284.77947	−284.93290	−284.84016	−284.99663	252
TS-CO2 **TS11**	−283.91735	−284.76811	−284.92023	−284.82714	−284.98265	238
PC-CC2 **12**	−283.97916	−284.80383	−284.95619	−284.86686	−285.02198	253
RC-CC2 **13**	−283.96053	−284.78538	−284.94014	−284.84701	−285.00460	235
TS-CC2 **TS14**	−283.90118	−284.75744	−284.90869	−284.81389	−284.96918	233
PC-CC2 **15**	−284.02139	−284.84316	−284.99296	−284.90423	−285.05743	246

[a] Based on HF/6-31G(d,p) geometries. [b] Based on MP2/6-31G(d,p) geometries. [c] Zero-Point Energies from HF/6-31G(d,p) and scaled by 0.9.

reported that an amide enol can be prepared in solution as relatively long-lived species whose NMR spectra can be recorded and analyzed, when bulky aryl groups confer on them kinetic stability. They did similar work on enols of carboxylic acid derivatives[9] which are also unstable species. The question of interest concerning the amination of ketenes is therefore whether the enol of the amide is formed in these cases[7,8] solely due to sterical effects of the bulky substituents or rather to intrinsic electronic effects. It is clear that a complete and detailed understanding of this amination reaction remains an unsolved problem and therefore some questions are of primary importance in the present study: (a) does addition of ammonia to ketene **a** occur in a concerted fashion and, if so, is this across the C=C or the C=O bond of the ketene. (b) If addition occurs formally across the C=O bond of ketene **a**, then the hemiaminals **b** are intermediates in the reaction—can these be isolated or observed in solution? Our experimental approach has been to search for such an intermediate, and therefore bulky aromatic groups as ketene substituents were incorporated in order to slow subsequent reactions. (c) Because in some experiments the amide formation reaction takes place in steam and excess NH_3 (or amines), it is appropriate to consider whether the catalyst is either H_2O or NH_3. Both possibilities will be discussed including gas phase and solvent calculations as well. Eventually, the reported results should permit some more meaningful discussion regarding the mechanism of carbonyl addition in condensed media, and their analysis provides insight into the nature of active catalysis.

Details of Calculations

Ab initio molecular orbital (MO) and density functional theory (DFT) methods are both used in modeling the amide bond formation. All calculations were carried out using the GAUSSIAN 94[10] set of programs. The stationary points of interest were initially located and characterized by harmonic vibrational analysis employing Hartree−Fock (HF) calculations with the dp-polarized 6-31G(d,p) basis set. Note that

the acronym n-ijG or n-ijkG can be encoded as: *n*, the number of primitives for the inner shells; ij or ijk, the number of primitives for contractions in the valence shell. The ij notation describes sets of valence double-ζ quality and ijk sets of valence triple-ζ quality. The relevant structures were then reoptimized at second-order Møller−Plesset perturbation theory (MP2) level with the same basis set. Improved relative energies between stationary points were finally estimated using the quadratic configuration interaction method (QCISD-(T)) with the 6-31G(d,p) and 6-311++G(d,p) basis set at MP2/6-31G(d,p)-optimized geometries (++ indicates a set of sp-diffuse functions on C, N, and O and s-diffuse functions on H). These relative values were also corrected for zero-point vibrational energies (ZPE) derived from HF/6-31G(d,p) calculations and scaled by 0.9. The understanding of the effect of solvation on reaction rates has been tackled employing different approaches. We initially assembled the reacting sphere using the supermolecule approach, in which the solvent molecules are considered explicitly. The supermolecule consists of a ketene molecule and some reacting solvent molecules (both NH_3 and H_2O), and quantum chemical calculations are performed for the whole system. All structures of interest were treated at the same levels of theory. A more appropriate treatment of solvation effects needs to include not only the influence of the active solvent, whose structure is modified by the presence of the solute, but also that of the bulk solvent. For the latter purpose, the solvent is represented by an infinite dielectric and polarizable continuum characterized by its dielectric constant (ϵ). In the present paper, the latter was estimated by different solvent models: the Onsager SCRF method,[11] the PCM model of Tomasi et al.,[12] and a SCRF approach, using the Self-Consistent Isodensity Polarized Continuum Model (SCI-PCM).[13] PCM models use apparent solvent charges resting on the surface of the solute to give access

(9) Frey, J.; Rappoport, Z. *J. Am. Chem. Soc.* **1995**, *117*, 1161.

(10) M. J.; Trucks, G. W.; Schlegel, H. B.; Gill, P. M. W.; Johnson, B. G.; Robb, M. A.; Cheeseman, J. R.; Keith, T.; Petersson, G. A.; Montgomery, J. A.; Raghavachari, K.; Al-Laham, M. A.; Zakrzewski, V. G.; Ortiz, J. V.; Foresman, J. B.; Cioslowki, J.; Stefanov, B. B.; Nanayakkara, A.; Challacombe, M.; Peng, C. Y.; Ayala, P. H.; Chen, W.; Wong, M. W.; Andres, J. L.; Replogle, E. S.; Comperts, R.; Martin, R. L.; Fox, D. J.; Binkley, J. S.; DeFrees, D. J.; Baker, J.; Stewart, J. J. P.; Head-Gordon, M.; Gonzalez, C.; Pople, J. A., Gaussian Inc., Pittsburgh, PA, 1995.

(11) Wong, M. W., Frisch, M. J.; Wiberg, K. B. *J. Am. Chem. Soc.* **1991**, *113*, 4776.

(12) Tomasi, J.; Persico, M. *Chem. Rev.* **1994**, *94*, 2027.

(13) Wiberg, K. B.; Castejon, H.; Keith, T. A. *J. Comput. Chem.* **1996**, *17*, 185.

Table 2. Calculated Relative Energies (kJ mol⁻¹) for the Amination of Ketenes, All Corrected by Zero-Point Vibrational Energies (ZPE, kJ mol⁻¹)
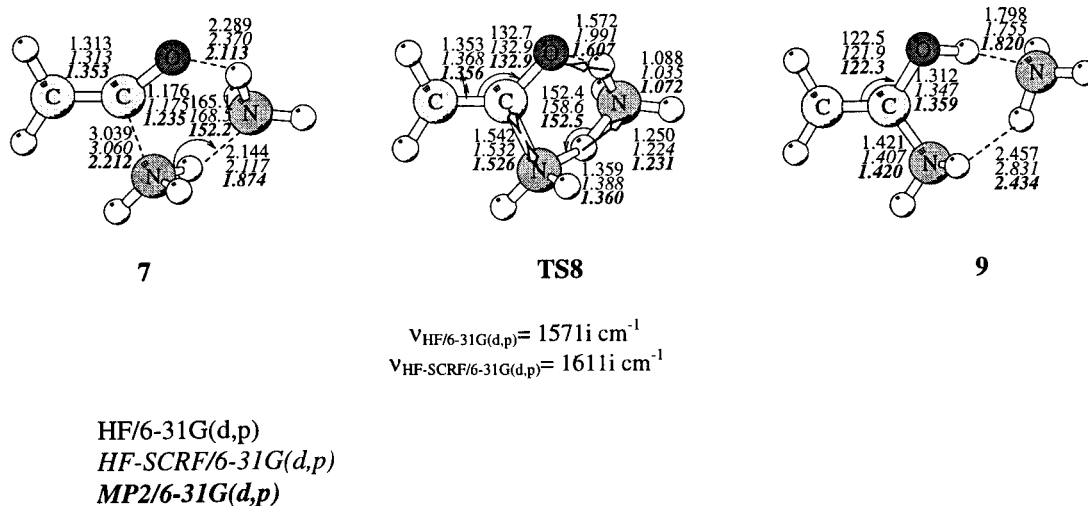
	HF[a] 6-31G(d,p)	MP2[b] 6-31G(d,p)	MP2[b] 6-311++G(d,p)	QCISD(T)[b] 6-31G(d,p)	QCISD(T)[b] 6-311++G(d,p)
$1 + NH_3$	0	0	0	0	0
TS-CC **TS2**	233	207	166	173	174
PC-CC **3**	−153	−111	−137	−151	−137
RC-CO **4**	−9	31	−10	−13	−11
TS-CO **TS5**	183	167	128	128	132
PC-CO **6**	−25	19	−22	−28	−25
$1 + 2 NH_3$	0	0	0	0	0
RC-CO1 **7**	45	50	6	2	10
TS-CO1 **TS8**	101	81	38	37	46
PC-CO1 **9**	−53	−13	−57	−67	−58
$1 + NH_3 + H_2O$	0	0	0	0	0
RC-CO2 **10**	43	45	10	0	12
TS-CO2 **TS11**	95	61	29	20	35
PC-CC2 **12**	−52	−18	−51	−69	−53
RC-CC2 **13**	−34	13	−26	−35	−26
TS-CC2 **TS14**	133	84	54	50	65
PC-CC2 **15**	−170	−128	−154	−174	−153

[a] Based on HF/6-31G(d,p) geometries. [b] Based on MP2/6-31G(d,p) geometries.

HF/6-31G(d,p)
HF-SCRF/6-31G(d,p)
HF-SCI-PCM/6-31G(d,p)
MP2/6-31G(d,p)
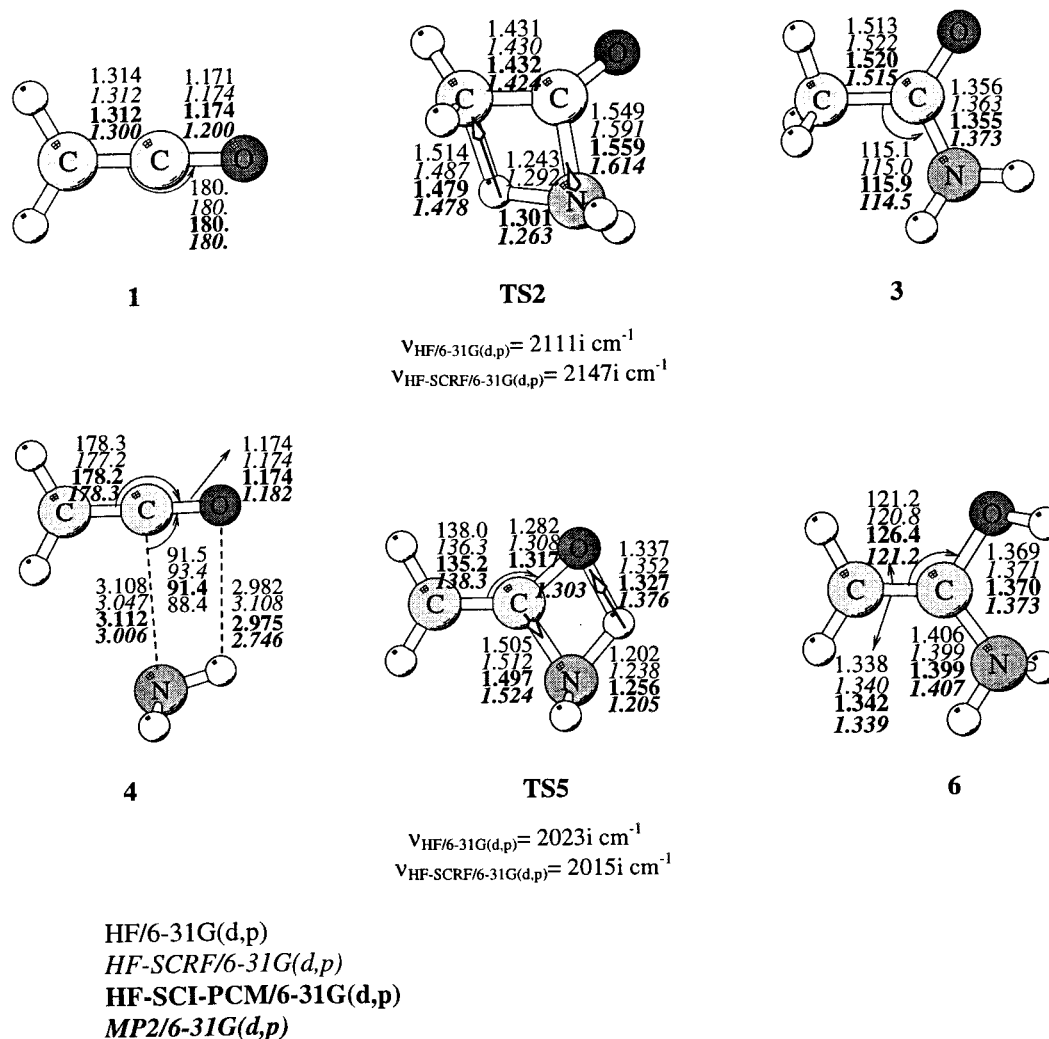
Figure 1. Optimized structures of the stationary points along the amination path of ketene with one NH_3 molecule ($H_2C=C=O + NH_3$) across both C=O and C=C bonds.

to the electrostatic part of the solvation free energy (electrostatic interactions between the solute and an external electric field, solvent polarization). Isodensity-PCM models define the cavity of the solute by its electron density through an isodensity level, rather than using regular bodies or combinations of them. The SCI-PCM model determines for its part the quantum description of the solute (wave function or electron density), the shape of the cavity, and the solvent charge distribution in a self-consistent manner rather than using an unperturbed gas-phase cavity. Self-consistency is determined by convergence of solvent charges. SCI-PCM optimization calculations were carried out using the DFT method with the
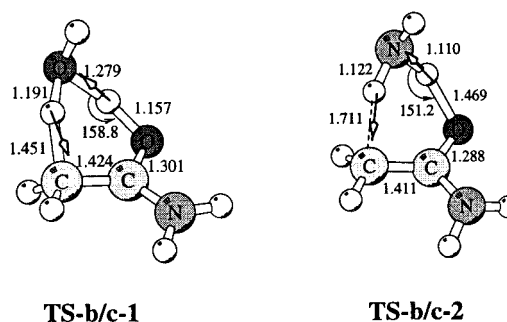
$\nu_{HF/6\text{-}31G(d,p)} = 1571i\ cm^{-1}$

$\nu_{HF\text{-}SCRF/6\text{-}31G(d,p)} = 1611i\ cm^{-1}$

HF/6-31G(d,p)
HF-SCRF/6-31G(d,p)
MP2/6-31G(d,p)

Figure 2. Optimized structures of the stationary points along the amination path of ketene with two NH_3 molecules ($H_2C=C=O$ + 2 NH_3) across the C=O bond.

B3LYP functional and the 6-31G(d,p) basis set and were based on gas-phase structures optimized at the same level of theory. Throughout this paper, bond lengths are given in angstroms, bond angles in degrees, total energies in hartree, zero-point and relative energies in kJ mol^{-1}.

Results and Discussion

Reaction Mechanism in Gas Phase. Reaction Profile for $H_2C=C=O + NH_3$. We have started our study investigating the reaction between ketene and a single ammonia to form an amide. To obtain information about the preferred interaction of ammonia with ketene, we have studied the reaction profile corresponding to attack of ammonia across both the C=O and C=C bonds of ketene. The calculated total and relative energies of the stationary points along the amination reaction paths are given in Tables 1 and 2, and geometrical features of the relevant structures are displayed in Figure 1. While complexation involving the C=O bond of the ketene **1** and an ammonia molecule occurred giving the cyclic complex **4** (Figure 1), ammonia does not form a cyclic complex with the C=C bond of ketenes. Probably, in the latter, bonds are too weak to form a "preassociation" complex as a starting point for the addition of ammonia across the C= C bond of ketene. Despite an intensive search on the potential energy surface, a zwitterion-like intermediate could not be located either in gas phase or in polar solvent continuum. Instead, cyclic transition structures for addition across both C=C **TS2** and C=O **TS5** bonds of the ketene were located and characterized. The most important feature of these transition structures is the remarkable energy difference between both reaction paths (see Tables 1 and 2). Note that RC stands for reactant complex, TS for transition structure, and PC for product complex; CO means addition across the C=O bond of ketene; CC concerns addition across the C=C bond of ketene. The higher energy of **TS2** can be attributed to the rotation of the CH_2 group in the ketene, which of course requires energy. In **TS2**, an additional distortion of the CH_2 moiety is forced. Due to this distortion, **TS2** lies about 42 kJ mol^{-1} higher in energy than **TS5**. To confirm that for the addition across C=O, the **a** → **b** path (ketene + ammonia → diol) is rate-determining, we traced the subsequent **b** → **c** step (enol
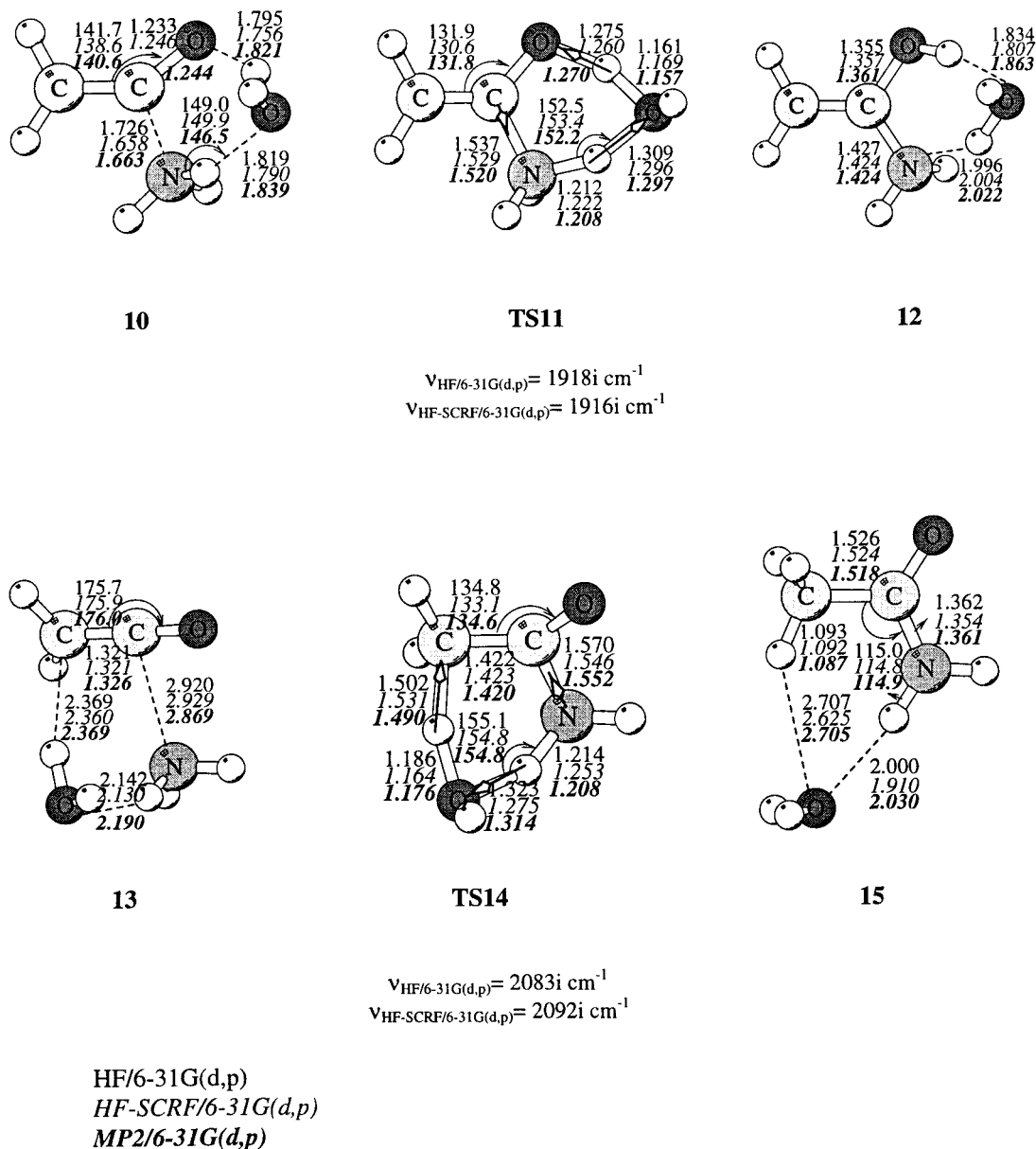
→ amide) as well (see Scheme 1). Calculations on the 1,3-H-shift connecting the enol and the amide include either an assisting water molecule (**TS-b/c-1**) or an assisting ammonia molecule (**TS-b/c-2**) to perform the proton transfer in a facile and rapid way. Both transition structures **TS-b/c-1** and **TS-b/c-2** were optimized at the MP2/6-31G(d,p) level of theory and are displayed below. Transition vectors at the HF/6-31G(d,p) level of theory are shown as well.

TS-b/c-1   **TS-b/c-2**

$\nu_{HF/6\text{-}31G(d,p)} = 2050i\ cm^{-1}$ $\nu_{HF/6\text{-}31G(d,p)} = 394i\ cm^{-1}$

$\nu_{HF\text{-}SCRF/6\text{-}31G(d,p)} = 592i\ cm^{-1}$ $\nu_{HF\text{-}SCRF/6\text{-}31G(d,p)} = 330i\ cm^{-1}$

At the QCISD(T)/6-31G(d,p) level of theory, the energy barrier for C=O addition tends to be 141 kJ mol^{-1}, which is about 107 kJ mol^{-1} larger than the one for the 1,3-H-shift assisted by a water molecule having an energy barrier of only 36 kJ mol^{-1} and 96 kJ mol^{-1} larger than the 1,3-H-shift assisted by an ammonia molecule. It turns out that the addition of C=O to ketene is the rate-controlling step, whereas the subsequent assisted 1,3-H-shift is only a low barrier step. Therefore, the 1,3-H-shift is not taken into account any further in this paper. As the activation energy for C=O addition is still very high, being 141 kJ mol^{-1} at high level of theory (QCISD-(T)/6-31G(d,p)+ZPE), it is suggested that the solvent plays a catalytic role.

Reaction Profile Using NH_3 as a Catalyst. To study the catalytic effect of a second amine molecule on this reaction, we have investigated the reaction profile

10 **TS11** **12**

$$\nu_{HF/6\text{-}31G(d,p)}= 1918i \text{ cm}^{-1}$$
$$\nu_{HF\text{-}SCRF/6\text{-}31G(d,p)}= 1916i \text{ cm}^{-1}$$

13 **TS14** **15**

$$\nu_{HF/6\text{-}31G(d,p)}= 2083i \text{ cm}^{-1}$$
$$\nu_{HF\text{-}SCRF/6\text{-}31G(d,p)}= 2092i \text{ cm}^{-1}$$

HF/6-31G(d,p)
HF-SCRF/6-31G(d,p)
MP2/6-31G(d,p)

Figure 3. Optimized structures of the stationary points along the amination path of ketene with both an NH_3 and a H_2O molecule ($H_2C=C=O + NH_3 + H_2O$) across both $C=O$ and $C=C$ bonds.

adding an extra ammonia molecule. Extensive search on the potential energy surface has led to the location of the RC **7** and TS **TS8**. Note that in many cases, preassociative complexes such as **7**, **10**, and **13** have been located. It turns out that, upon incorporation of zero-point vibrational energies, the enthalpies of these complexes become higher than those of the fragments. Whether or not these complexes exist, their nuclear configuration certainly plays an important role in the early stage of the addition. Inspection of the structural data reported in Figure 2 for **TS8** shows that this saddle point corresponds to a rather asynchronous TS, the distances O−H and H−N being 1.607 and 1.072 Å, respectively. The added NH_3 molecule forms two hydrogen bonds with the ketene and the original NH_3 molecule in a cyclic complex. **TS8** apparently corresponds to an addition in two planes: while a nitrogen atom of the ammonia dimer attacks the central C_α atom in the molecular plane of ketene, a hydrogen atom is transferred to the oxygen of ketene in a quasiperpendicular plane

(cf. Figure 2). We also note that no significant distortion of the CH_2 group is involved in the addition processes. All our attempts to locate a TS across the $C=C$ bond of ketene failed. The calculated energy barrier for the **7** → **TS8** → **9** reaction is found to be only 36 kJ mol^{-1} at the QCISD(T)/6-311++G(d,p) level. Such values reflect well the catalytic effect of a second reactant molecule. Thus, the calculated decrease in activation energy with respect to the parent transformation **4** → **TS5** → **6** is 107 kJ mol^{-1} at the same level of theory.

The Reaction Profile Using H_2O as a Catalyst. Chains composed of an extra amine molecule will perform the amination with only a low barrier. However, as the amide bond forming reaction takes place in steam and excess amine, that means with a certain presence of water, it is appropriate to find out whether the catalyst is either H_2O or amine. To probe this, calculations were performed to locate stationary points including an additional water molecule as a proton relay. Figure 3 shows the relevant stationary points for ammonia addition to

Table 3. Activation Energies (kJ mol^{-1}) for the Amination of Ketenes, Including Different Numbers of Solvent Molecules

	HF[a] 6-31G(d,p)	MP2[b] 6-31G(d,p)	MP2[b] 6-311++G(d,p)	QCISD(T)[b] 6-31G(d,p)	QCISD(T)[b] 6-311++G(d,p)
1 + NH$_3$ (CO)	192	136	138	141	143
1 + NH$_3$ (CC)	233	207	166	173	174
1 + 2 NH$_3$ (CO)	56	31	32	35	36
1 + NH$_3$ + H$_2$O (CO)	52	16	19	20	23
1 + NH$_3$ + H$_2$O (CC)	167	71	80	85	91

[a] Based on HF/6-31G(d,p) geometries. [b] Based on MP2/6-31G(d,p) geometries.

ketene across both C=O and C=C bonds assisted by a water molecule which participates bifunctionally in cyclic structures. In this case, both preassociating complexes **10** and **13** and TS's **TS11** and **TS14** can be formed. The activation energies, given in Table 3, show a dramatic reduction in the barrier height compared to the uncatalyzed addition upon the introduction of a water molecule. The water molecule in **TS11** acts classically as a proton donor in a hydrogen bond to ketene and as a proton acceptor to the ammonia molecule. From Table 3, it is clear that the water-assisted reaction across the C=O bond of ketene is largely preferred above the one across the C=C bond. An energy barrier of only 23 kJ mol^{-1} is found for the former, which means a further reduction of 13 kJ mol^{-1} relative to the addition of the ammonia dimer. This can be understood in terms of the stronger proton-donating character of water compared to ammonia, which yields an almost completed TS. A closer look at transition structures **TS8** and **TS11** confirms this fact. In **TS11**, the proton transfer from water to the oxygen of ketene is almost achieved (1.270 Å), whereas the proton of ammonia in **TS8** has not moved yet to the ketene (1.607 Å). A similar observation on the preference of H$_2$O as catalyst has been reported earlier in the neutral 1,1-addition to isocyanides.[14] In any case, it is apparent that if a dimer of amine or a amine−water complex could be involved in the reaction, an almost barrier-free amination could occur at the C=O moiety, producing the primary enol of amide. Finally, an association of two water molecules plus an ammonia molecule with the ketene has been investigated. Both the associated complex **16** and the subsequent transition structure **TS17** are displayed below, its geometry being optimized at the MP2/6-31G(d,p) level of theory. The energy barrier for this reaction tends to be 35 kJ mol^{-1} at the MP2/6-311++G(d,p) //MP2/6-31G(d,p)+ZPE level of theory. This value is in line with both the reactions including one ammonia plus one water molecule and two ammonia molecules. Nevertheless, the energy barrier for inclusion of a second water molecule seems to be somewhat larger than the one with only one water molecule. This fact points out that addition of another water molecule does not catalyze the reaction any further, but rather slows down the reaction by a small extent. The latter can be understood by steric hindrance and less efficient hydrogen transfer occurring when the cluster size grows. This case is therefore not considered any further in the present paper.

Reaction Mechanism in Solvent. The next step in our investigation was to study the solvent effect on the basic features of the reaction and to compare these features with those observed for the gas phase. First we
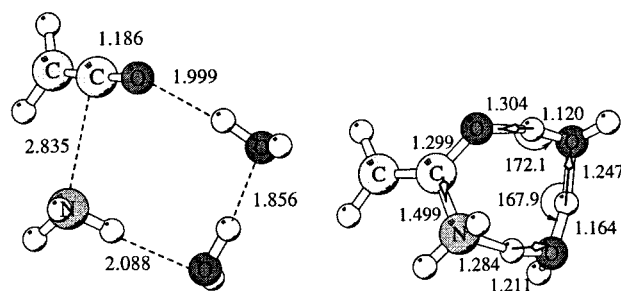
16   **TS17**

$\nu_{HF/6\text{-}31G(d,p)} = 913i\ cm^{-1}$

$\nu_{HF\text{-}SCRF/6\text{-}31G(d,p)} = 869i\ cm^{-1}$

have reoptimized the stationary points **1**−**15** using the Onsager model as implemented in Gaussian 94. The geometric features are shown in Figures 1−3. The total, zero-point vibrational and relative energies are summarized in Tables 4 and 5. Inspection of these data indicates that the electrostatic solvation energies computed using the Onsager model stabilize similarly the reactants **1**, **4**, **7**, **10**, **13**, products **3**, **6**, **9**, **12**, **15**, and transition structures **TS2**, **TS5**, **TS8**, **TS11**, **TS14**. As a consequence, the activation and reaction energies do not vary significantly from those obtained in the gas phase. To find out whether the rather drastic simplifications introduced in the Onsager model could cause an incorrect description of the reaction profile, we have reoptimized the stationary points **1**−**6** using the more sophisticated SCI-PCM method. The energies of these stationary points can again be found in Tables 4 and 5, and structural features are displayed in Figure 1. Our results indicate that the profile of the reaction does not change significantly when a more elaborate model of the solute−solvent interaction is used. The optimized geometries are comparable to those obtained with the Onsager model. Therefore, these CPU-intensive calculations were not extended to the larger dimeric systems in which the gas phase reaction is virtually spontaneous.

Experimental Evidence for the Formation of Enols of Amides in the Amination of Ketene. Having established theoretically the preference of the two-step reaction path across the C=O bond generating the primary enols of amides, we now report the experimental evidence. This kinetic investigation was carried out using sterically hindered ketenes, namely bis(pentamethylphenyl) ketene (PMP)$_2$C=C=O and bis(mesityl) ketene by a range of primary, secondary, and tertiary amines. The preparation of ketenes is described by Allen et al.[15] Diketene formation is excluded by the experimental conditions, since the concentration of ketene present is generally <10^{-5} M. The UV spectrum of the ketenes

(14) Nguyen, M. T.; Hegarty, A. F. *J. Chem. Soc., Perkin Trans 2* **1987**, 1675.

**Table 4. Total Energies (hartree) of the Considered Stationary Points, Both in Gas Phase ($\epsilon = 1$) and Solvent ($\epsilon = 78.3$), Using the PCM, SCRF, and SCI-PCM Solvent Method**

| | gas phase | | solution | | |
	MP2	B3LYP	MP2 PCM	B3LYP SCRF	B3LYP SCI-PCM
$H_2C=C=O$ **1**	−152.17629	−152.60202	−152.16480	−152.60299	−152.60504
NH_3	−56.38692	−56.55777	−56.39338	−56.55989	−56.56332
H_2O	−76.22245	−76.41974	−76.23051	−76.42310	−76.42814
1 + NH_3	−208.56321	−209.15979	−208.55818	−209.16288	−209.16836
TS-CC **TS2**	−208.48615	−209.10330	−208.49598	−209.10710	−209.11452
PC-CC **3**	−208.61178	−209.22322	−208.62555	−209.22749	−209.23461
RC-CO **4**	−208.55311	−209.16557	−208.55850	−209.16679	−209.17100
TS-CO **TS5**	−208.50289	−209.11917	−208.52300	−209.12756	−209.13515
PC-CO **6**	−208.56399	−209.17819	−208.57605	−209.18001	−209.18731
1 + 2 NH_3	−264.95013	−265.71756	−264.95156	−265.72270	−
RC-CO1 **7**	−264.94029	−265.73423	−264.96096	−265.73473	−
TS-CO1 **TS8**	−264.92719	−265.71896	−264.95054	−265.73325	−
PC-CO1 **9**	−264.96585	−265.75456	−264.97943	−265.75996	−
1 + NH_3 + H_2O	−284.78566	−285.57953	−284.78869	−285.58598	−
RC-CO2 **10**	−284.77947	−285.59603	−284.80308	−285.60055	−
TS-CO2 **TS11**	−284.76811	−285.58706	−284.78956	−285.59199	−
PC-CC2 **12**	−284.80383	−285.61855	−284.81948	−285.62052	−
RC-CC2 **13**	−284.78538	−285.59757	−284.80191	−285.59759	−
TS-CC2 **TS14**	−284.75744	−285.57632	−284.77760	−285.57944	−
PC-CC2 **15**	−284.84316	−285.65485	−284.86761	−285.66652	−

Table 5. Relative Energies (kJ mol^{-1}) of the Considered Stationary Points, Both in Gas Phase ($\epsilon = 1$) and Solvent ($\epsilon = 78.3$), Using the PCM, SCRF, and SCI-PCM Solvent Method

| | gas phase | | solution | | |
	MP2	B3LYP	MP2 PCM	B3LYP SCRF	B3LYP SCI-PCM
1 + NH_3	0	0	0	0	0
TS-CC **TS2**	207	152	168	166	145
PC-CC **3**	−111	−148	−160	−151	−155
RC-CO **4**	31	−10	3	−1	−2
TS-CO **TS5**	167	115	101	101	95
PC-CO **6**	19	−40	−26	−37	−42
1 + 2 NH_3	0	0	0	0	−
RC-CO1 **7**	50	−31	−1	−25	−
TS-CO1 **TS8**	81	14	21	−10	−
PC-CO1 **9**	−13	−68	−45	−69	−
1 + NH_3 + H_2O	0	0	0	0	−
RC-CO2 **10**	45	−15	−9	−10	−
TS-CO2 **TS11**	61	−2	13	2	−
PC-CC2 **12**	−18	−70	−51	−59	−
RC-CC2 **13**	13	−32	−23	−15	−
TS-CC2 **TS14**	84	23	39	32	−
PC-CC2 **15**	−128	−171	−184	−184	−

studied is very characteristic with λ_{max} = 254 nm. The reaction of $PMP_2C=C=O$ with morpholine is characterized by the formation of an intermediate (λ_{max} = 300 nm) (Figure 4a) and by its subsequent decay (Figure 4b). Addition of amines (e.g., piperidine or morpholine) to a solution of $(Mes)_2C=C=O$ in chloroform in a IR cell yielded a peak at 1616 cm^{-1}. In time this peak weakened, with the simultaneous formation of the amide carbonyl peak at 1641 cm^{-1} (Figure 5). The IR absorbance at 1616 cm^{-1} is characteristic of a C=C bond with electron-donating substituents. The similarity of these findings with those of the hydrolysis of ketenes[15] suggests that the reaction of amines with ketenes **a** occurs via the same process, i.e., formation of the enol of the amide intermediate **b** with subsequent ketonization of the amide **c**:
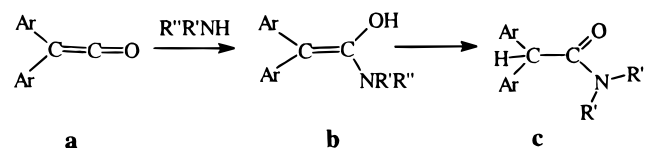
(15) Allen, B. M.; Hegarty, A. F.; O'Neill, P.; Nguyen, M. T. *J. Chem. Soc., Perkin Trans 2* **1992**, 927.
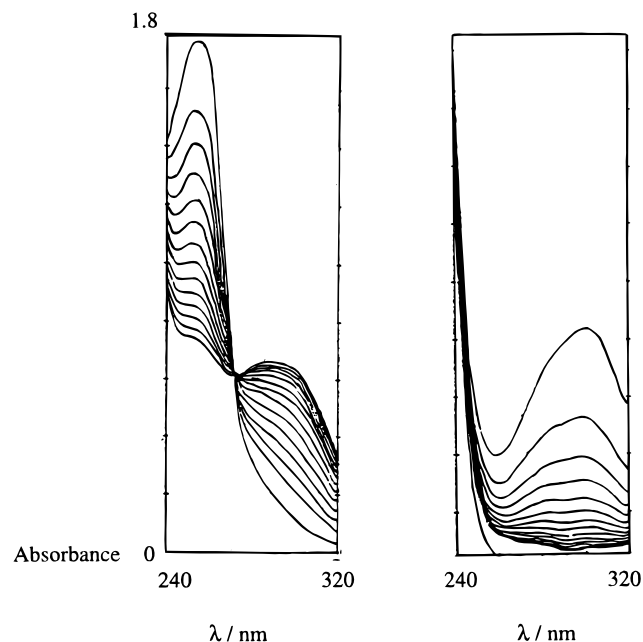

Figure 4. (a) Repetitive scans of the UV region for formation of the enol of amide from $PMP_2C=C=O$ and morpholine in acetonitrile. Morpholine (0.5 μL) was added to 2 mL of $PMP_2C=C=O$ (10^{-4} M) in acetonitrile. (b) Repetitive scans of the UV region for ketonization of the enol of amide, $PMP_2C=C(OH)(NC_4H_8O)$, formed by the addition of 10 μL morpholine to 2 mL of $PMP_2C=C=O$ (10^{-4} M) in acetonitrile. Intervals between scans, 50 s.

The above behavior holds true for both primary and secondary amines. However, tertiary amines give a slightly different effect involving slower reaction as would be expected due to the absence of a proton for ketonization.

Mechanism of Amination. From the plots of k_{obs} versus [amine] (Figure 6), we see that the rate dependence is first-order in amine concentration, over the concentration range studied. This is consistent with a mechanism for amination which involves rate-determining nucleophilic attack on the C_α of the ketene initially yielding an enol of the amide. As seen in the theoretical results, such a path is associated with a smaller activation energy. We therefore propose that the amination

Table 6. Activation Energies (kJ mol⁻¹) for the Amination of Ketenes, Including Electrostatic Effects of the Solvent

	gas phase		solution		
	MP2	B3LYP	MP2 PCM	B3LYP SCRF	B3LYP SCI-PCM
$H_2C{=}C{=}O + NH_3$ (CO)	136	125	98	102	97
$H_2C{=}C{=}O + NH_3$ (CC)	207	152	168	166	145
$H_2C{=}C{=}O + 2\ NH_3$ (CO)	31	45	22	15	–
$H_2C{=}C{=}O + NH_3 + H_2O$ (CO)	16	13	22	12	–
$H_2C{=}C{=}O + NH_3 + H_2O$ (CC)	71	55	62	47	–
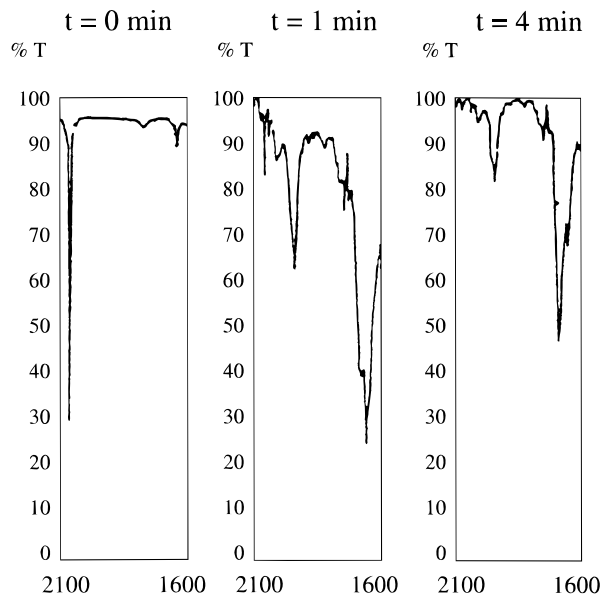
Figure 5. IR spectra recorded at intervals of time during the reaction of $Me_2C{=}C{=}O$ with morpholine in chloroform solution. Absorbance at 1925 cm⁻¹ is due to morpholine.
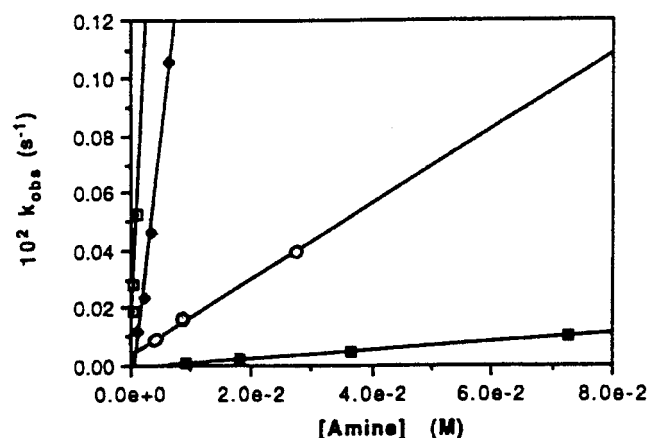
Figure 6. Plot of the observed rates versus [amine] for the addition of several amines to $Mes_2C{=}C{=}O$. (▫) Piperidine; (◆) morpholine; (○) *N*-methylmorpholine; (■) *N*-ethylpiperidine.

of ketenes proceeds via amine addition across the C=O bond rather than the C=C bond. Lillford and Satchell[5] accepted that a carbonyl addition mechanism could conceivably satisfy all their data leading to the formation of the enol of the amide intermediate but discounted this mechanism as unlikely due to the need for a rapid subsequent prototropic rearrangement. In this regard, we have not considered here the second step of amide bond formation, but it is well established that the enol–ketene isomerization is a rather fast process (crf. **TSb/c-1** and **TSb/c-2**). Tidwell[10] argued that the higher reactivity of diphenylketene, relative to dialkylketenes,

favors the open transition states due to the ability of the phenyl ring to stabilize the negative charge which develops at C_β. As for a counter-argument, we refer to the calculated results summarized in Table 4 that show that the TS for C=O addition is invariably lower in energy than the TS for C=C, irrespective of the reaction condition (in gas phase or in solution; with or without solvent assistance). It is worth noting that even in highly polar solution ($\epsilon = 78$), the TS for C=C addition **TS2** is much less stabilized than the C=O counterpart **TS5**. Apparently, a negative polarization at C_β, if any, does not take much advantage from the solvent whose effect is expected to be much larger in such circumstances than that of substituents. Moreover, it seems difficult to conceive of an "open TS" under these circumstances. The migrating hydrogen needs to be placed somewhere in an appropriate position near the negative end in order to be transferred after the TS is passed on the reaction coordinate. A hydrogen bond type interaction is then expected to develop, and the corresponding TS is rather closed than open. The preference for a TS (C=O) like **TS5** over a TS (C=C) like **TS2** has been discussed in detail in earlier papers on ketene hydration.[15,16] It may also be argued that an addition across the C=O moiety could not account for the observed decrease in reactivity with increasing steric bulk. We note that the orientation of the substituents on the aryls extends the steric bulk toward C_α in such a way that in-plane attack involving the carbonyl group (C=O) might be retarded significantly.

Our proposed mechanism is also not in conflict with the absence of the involvement of an amine dimer. It is already known that these amine dimers are likely to be present in solution in low concentrations with respect to free amine. The reactivity of these dimers with our sterically hindered ketenes would be much slower than the reaction of free amine and may explain the nonexistence of a second-order rate term in our kinetic analysis. Calculated results discussed above also show the preference, when water is present, of an amine-water complex over the amine dimer, as reactants.

Conclusions

In the present paper, a kinetic and mechanistic study of the addition of amine to ketene has been undertaken. Both experimental and theoretical results consistently show that the amination of ketene should be understood as a two-step reaction involving an enol of an amide as an intermediate (addition of amine across the C=O bond of ketene), rather than as a concerted mechanism involving addition across the C=C bond of the ketene. Moreover, it is seen that active catalysis by specifically interacting protic solvent molecules represents an ef-

(16) Nguyen, M. T.; Hegarty, A. F. *J. Am. Chem. Soc.* **1984**, *106*, 1552.

ficient way to make an amide bond. The amination reaction involves simultaneous nucleophilic attack of the amine on the ketene carbonyl carbon, and transfer of a hydrogen atom to the ketene oxygen, with the assistance of a second amine, leading to six-membered ring transition states. Water instead of a second amine molecule catalyzes the reaction even more efficiently with a more compact TS. The preferred addition across the C=O bond of ketene pointed out by calculations is in accordance with the kinetic evidence now presented for the formation of enols of amides. The latter were generated as intermediates in the amination of the sterically hindered ketenes, $(PMP)_2C=C=O$ and $(Mes)_2C=C=O$, by primary and secondary amines. However, for these specific ketenes, the kinetics of formation of the enol of the amide shows a first-order dependency on amine concentration, and the rates of addition of several amines to $(PMP)_2C=C=O$ and $(Mes)_2C=C=O$ have been determined. The first-order dependency on amine concentration suggests a reaction involving free amine molecules rather than dimers. This is on one hand not in conflict with the theoretical results and points out on the other hand the importance of steric hindrance in these systems.

Note Added in Proof. A recent theoretical study (Sung, K.; Tidwell, T. T. *J. Am. Chem. Soc.* **1998**, *120*, 3043) on the amination of ketene using MP2/6-31G(d) calculations also showed the preference of the addition of NH_3, $(NH_3)_2$, and NH_3-H_2O) to the C=O bond of ketene over that to the C=C bond.

JO980642T